

## Statistical Moments and Scintillation Level of Scattered Electromagnetic Waves in the Magnetized Plasma

George Jandieri<sup>1, \*</sup>, Akira Ishimaru<sup>2</sup>, Banmali Rawat<sup>3</sup>,  
Vladimir Gavrilenko<sup>4</sup>, and Oleg Kharshiladze<sup>5</sup>

**Abstract**—Statistical characteristics of scattered ordinary and extraordinary electromagnetic waves in the magnetized plasma are considered using the smooth perturbation method. Diffraction effects and polarization coefficients are taken into account. Second order statistical moments of scattered radiation are obtained for arbitrary correlation function of electron density fluctuations. The expressions of the broadening of the spatial power spectrum and displacement of its maximum are obtained. Wave structure functions and the angle of arrivals are calculated. Scintillation level of scattered radiation is analyzed for different parameters characterizing anisotropic plasma irregularities for the ionospheric F-region. Numerical calculations of the statistical characteristics are carried out for the three-dimensional spectral function containing anisotropic Gaussian and power-law spectral functions using the experimental data.

### 1. INTRODUCTION

At the present time peculiarities of electromagnetic (EM) waves propagation in a randomly inhomogeneous media have been rather well studied [1, 2]. The analysis of the statistical properties of small-amplitude electromagnetic waves that pass through a plane turbulent plasma slab is very important in many practical applications associated with both in natural and laboratory plasmas.

Many excellent reviews and books devoting to the scintillation theory and observations in the ionosphere have been published [3–5], whereas statistical characteristics of scattered radiation in the turbulent magnetized plasma are less studied. In most papers, isotropic irregularities have been considered; however, geomagnetic field leads to the birefringence and anisotropy.

The fluctuations in amplitude and phase (scintillation) of radio waves propagating through the ionosphere are caused by plasma irregularities in the electron density. The irregularities have different spatial scales and usually are elongated in the magnetic field direction. Ionospheric scintillation models contain the worldwide climatology of the ionospheric plasma density irregularities that cause scintillation, coupled to a model for the effects of these irregularities on radio signals. These irregularities distort the original wave front, giving rise to a randomly phase-modulated wave. A high priority given to the ionospheric scintillation study comes from its significant impact on satellite radio communications. For instance, the signal distortion caused by scintillation can degrade the performance of navigation system and generate errors in received messages.

Peculiarities of the second order statistical moments of scattered radiation in the collision magnetized plasma have been investigated in [6] using the ray (-optics) approximation. Statistical

---

*Received 6 March 2018, Accepted 26 April 2018, Scheduled 7 May 2018*

\* Corresponding author: George Jandieri (georgejandieri7@gmail.com).

<sup>1</sup> Georgian Technical University, Institute of Cybernetics, 77 Kostava Str., Tbilisi 0175, Georgia. <sup>2</sup> Department of Electrical Engineering, University of Washington, FT-10 Seattle, Washington 98 195, USA. <sup>3</sup> Department of Electrical and Biomedical Engineering, University of Nevada, Reno, USA. <sup>4</sup> Lobachevsky State University, Gagarin Av., 23, Nizhni Novgorod 630950, Russia.

<sup>5</sup> Tbilisi State University, Chavchavadze Ave. 3, Tbilisi 0179, Georgia.

characteristics and the scintillation level of scattered ordinary and extraordinary waves in the collision magnetized plasma normal to the external magnetic field have been considered in [7–10] using modified smooth perturbation method. Analytical and numerical calculations were carried out for both the anisotropic Gaussian and power-law spectral functions assumption taking into account diffraction effects. Scintillation index was calculated for small-scale irregularities using the “frozen-in” assumption and taking into account movement of rigid irregularities. Minimums of the power spectrum of intensity fluctuations of scattered ordinary and extraordinary waves satisfy the “standard relationship”. It was shown that the normalized scintillation level increases in both non-fully-developed diffraction pattern and transition zone increasing anisotropy factor. Rising orientation angle the scintillation level decreases, and splashes arise in a fully developed scintillation region.

In Section 2 of this paper, stochastic differential equation of the phase fluctuation has been obtained in the main plane containing wave vector of an incident wave and the external magnetic field. Polarization coefficients and diffraction effects are taken into account. In Section 3, second order statistical moments of scattered radiation are calculated for arbitrary correlation function of electron density fluctuations. Numerical calculations are carried out for new spectral function combining anisotropic Gaussian and power-law spectral functions in Section 4 using experimental data applied to the ionospheric  $F$ -region. In Section 5 normalized scintillation level is calculated for different anisotropy factors and orientation angles of elongated plasma irregularities with respect to the external magnetic field. Conclusion is presented in Section 6.

## 2. FORMULATION OF THE PROBLEM

Let a plane electromagnetic (EM) wave with frequency  $\omega$  be incident from vacuum on a semi-infinite slab of turbulent collisionless magnetized plasma. We choose a Cartesian coordinate system such that  $XY$  plane is the vacuum-plasma boundary;  $Z$  axis is directed in the plasma slab coinciding with the wave vector  $\mathbf{k}$  of the refracted wave;  $YZ$  plane (main plane) is generated by the external magnetic field vector  $\mathbf{H}_0$ . Components of the second rank permittivity tensor of the collisionless magnetized plasma are [11]:

$$\begin{aligned} \varepsilon_{xx} &= 1 - Y, & \varepsilon_{yy} &= 1 - Y(1 - u_T), & \varepsilon_{zz} &= 1 - Y(1 - u_L), & \varepsilon_{xy} &= -\varepsilon_{yx} = iY\sqrt{u_L}, \\ \varepsilon_{yz} &= \varepsilon_{zy} = Y\sqrt{u_L u_T}, & \varepsilon_{xz} &= -\varepsilon_{zx} = -iY\sqrt{u_T}, \end{aligned} \quad (1)$$

where  $Y = v/(1 - u)$ ,  $v(\mathbf{r}) = \omega_p^2(\mathbf{r})/\omega^2$  and  $u = \Omega_H^2/\omega^2$  are magneto-ionic parameters;  $\omega_p(\mathbf{r}) = [4\pi N(\mathbf{r})e^2/m]^{1/2}$  is the plasma frequency;  $\Omega_H = eH_0/mc$  is the angular gyrofrequency for the magnetic field;  $N(\mathbf{r})$  is the electron density;  $c$  is the speed of light in vacuum;  $e$  and  $m$  are the charge and mass of an electron, respectively;  $u_T = u \sin^2 \alpha$ ,  $u_L = u \cos^2 \alpha$ ,  $\alpha$  is the angle between  $\mathbf{k}$  and  $\mathbf{H}_0$  vectors. In reality components of the tensor  $\varepsilon_{ij}$  vary weakly on a distances of wavelength. We will consider distances  $L$  satisfying the condition  $L/kl^2 \ll 1$  ( $l$  is the characteristic spatial scale of irregularities). In a particular case of plane-layered medium, when components of the permittivity tensor  $\varepsilon_{ij}$  depend on one coordinate, the obtained results are valid for arbitrary distances.

Assuming  $\varepsilon_{ik}$  to be time independent, electric field  $\mathbf{E}$  in the turbulent magnetized plasma satisfies the differential equation:

$$\left( \frac{\partial^2}{\partial x_i \partial x_j} - \Delta \delta_{ij} - k_0^2 \varepsilon_{ij}(\mathbf{r}) \right) \mathbf{E}_j(\mathbf{r}) = 0, \quad (2)$$

where  $\Delta$  is the Laplacian,  $\delta_{ij}$  the Kronecker symbol, and  $k_0 = \omega/c$  the wavenumber of an incident wave.

Electric field that we introduce in [12, 13]  $E_j(\mathbf{r}) = E_{0j} \exp(\varphi_1 + ik_\perp y + ik_0 z)$  ( $k_\perp \ll k_0$ ), and  $k_\perp$  is the wavenumber normal to the main plane. Permittivity tensor  $\varepsilon_{ij}(\mathbf{r}) = \varepsilon_{ij}^{(0)} + \varepsilon_{ij}^{(1)}(\mathbf{r})$ ,  $|\varepsilon_{ij}^{(1)}(\mathbf{r})| \ll 1$  contains two terms. The first is a regular term, and the second is proportional to the complex phase  $\varphi_1 \sim \varepsilon_{ij}^{(1)}$ . Parameter  $\mu = k_\perp/k_0$  describes diffraction effects in a randomly inhomogeneous medium.

The first approximation fluctuation of the phase satisfies differential equation:

$$\left[ \nabla_i \nabla_j \varphi_1 + \nabla_i \varphi_0 \nabla_j \varphi_1 + \nabla_i \varphi_1 \nabla_j \varphi_0 - \delta_{ij} \left( \Delta_\perp + 2ik_\perp \frac{\partial \varphi_1}{\partial y} + 2ik_0 \frac{\partial \varphi_1}{\partial z} \right) - k_0^2 \varepsilon_{ij}^{(0)} \right] E_{0j} = 0. \quad (3)$$

where  $\Delta_{\perp} = (\partial^2 \varphi_1 / \partial x^2) + (\partial^2 \varphi_1 / \partial y^2)$  is the transversal Laplasian.

Substituting two-dimensional spectral function

$$\varphi_1(x, y, z) = \int_{-\infty}^{\infty} dk_x \int_{-\infty}^{\infty} dk_y \psi(k_x, k_y, z) \exp(ik_x x + ik_y y)$$

into Equation (3) we obtain:

$$\begin{aligned} & \frac{\partial \psi}{\partial z} + \frac{i}{k_x + (k_y + k_{\perp})} \frac{E_{0y}}{E_{0x}} \left[ k_0 k_x + k_0 k_y \frac{E_{0y}}{E_{0x}} - (k_x^2 + k_y^2 + 2k_{\perp} k_y) \frac{E_{0z}}{E_{0x}} \right] \psi \\ & = -i \frac{k_0^2}{k_x + (k_y + k_{\perp})} \frac{E_{0y}}{E_{0x}} \cdot \left( -i \hat{\varepsilon}_{zx}^{(1)} + \varepsilon_{yz}^{(1)} \frac{E_{0y}}{E_{0x}} + \varepsilon_{zz}^{(1)} \frac{E_{0z}}{E_{0x}} \right). \end{aligned} \quad (4)$$

where  $\hat{\varepsilon}_{zx}^{(1)} = \alpha_1 n_1(\mathbf{r})$ ,  $\varepsilon_{yz}^{(1)} = \alpha_2 n_1(\mathbf{r})$ ,  $\varepsilon_{zz}^{(1)} = -\alpha_3 n_1(\mathbf{r})$ ,  $\Psi \equiv v_0 / (1 - u_0)$ ,  $\alpha_2 = u_0 \Psi \sin \alpha \cos \alpha$ ,  $\alpha_1 = \sqrt{u_0} \Psi \sin \alpha$ ,  $\alpha_3 = \Psi (1 - u_0 \cos^2 \alpha)$ , electron density  $n_1(\mathbf{r})$  is random function of the spatial coordinates;  $k_x$  and  $k_y$  are the spatial wave-numbers in the  $x$  and  $y$  directions, respectively.

The ratio of the mean electric field components is expressed via well-known polarization coefficients:  $(E_{0y}/E_{0x}) = iP_j$ ,  $(E_{0z}/E_{0x}) = i\Gamma_j$  [11]:

$$P_j = \frac{2\sqrt{u_L}(1-v)}{u_T \pm \sqrt{u_T^2 + 4u_L(1-v)^2}}, \quad \Gamma_j = -v\sqrt{u_T} \frac{1 + P_j \sqrt{u_L}}{1 - u - v + vu_L}, \quad (5)$$

upper sign and index  $j = 1$  correspond to the extraordinary wave, and lower sign and index  $j = 2$  to the ordinary wave. These waves in magnetized plasma generally are elliptically polarized. Geomagnetic field leads to the birefringence and anisotropy.

Fluctuation of the phase of scattered electromagnetic wave caused by electron density fluctuations satisfies the boundary condition  $\varphi_1(k_x, k_y, z = 0) = 0$ . Applying the modified perturbation method [12, 14] the solution of Equation (4) is:

$$\psi(k_x, k_y, L) = A \int_0^L dz' (b_3 + ib_4) n_1(k_x, k_y, z') \exp[-\Upsilon(b_1 + ib_2)(L - z')], \quad (6)$$

where:  $A = (-\alpha_1 + P\alpha_2 + \Gamma\alpha_3) / \mu^2 P^2$ ,  $b_1 = \Upsilon k_x [k_0^2 \mu P - \Gamma(k_x^2 + k_y^2 + 2k_0 \mu k_y)]$ ,  $\Upsilon = 1/k_0^2 \mu^2 P^2$ ,  $b_2 = \Upsilon \{k_0 k_x^2 + P(k_y + k_0 \mu) [P k_0 k_y + \Gamma(k_x^2 + k_y^2 + 2k_0 \mu k_y)]\}$ ,  $b_4 = \Upsilon k_0^2 (k_y + k_0 \mu) P$ ,  $b_3 = \Upsilon k_0^2 k_x$ ,  $L$  is a propagation distance by electromagnetic waves in the ionospheric plasma. For simplicity, index  $j$  will be withdrawn from the polarization coefficients.

### 3. SECOND ORDER STATISTICAL MOMENTS OF SCATTERED RADIATION

Knowledge of the spectral function of the phase fluctuation allows the calculation of second order statistical moments of scattered electromagnetic waves. Using the Fourier transform of Equation (6) the variance of the phase fluctuations is:

$$\langle \varphi_1^2 \rangle = 2\pi A^2 \int_{-\infty}^{\infty} dk_x \int_{-\infty}^{\infty} dk_y (-B_0 + iB_1) W_n[k_x, k_y, \Upsilon(iB_3 - B_5)], \quad (7)$$

where  $B_0 = k_x^2 + P^2(-k_y^2 + k_0^2 \mu)^2$ ,  $B_1 = 2Pk_x k_y$ ,  $B_3 = k_x [k_0^2 \mu P - \Gamma(k_x^2 + k_y^2)]$ ,  $B_5 = Pk_y [-\Gamma(k_x^2 + k_y^2) + P\mu k_0^2 + 2\Gamma\mu^2 k_0^2]$ ,  $W_n(\mathbf{k})$  is the arbitrary correlation function of electron density fluctuations, and angular brackets mean ensemble average.

Correlation function between two observation points spaced apart at small  $\rho_y$  and  $\rho_x$  distances in the main and perpendicular planes, respectively, can be written in the form:

$$\begin{aligned} V_\varphi(\eta, L) &\equiv \langle \varphi_1(\mathbf{r}) \varphi_1^*(\mathbf{r} + \eta) \rangle \\ &= 2\pi A^2 k_0^4 L \int_{-\infty}^{\infty} dx \int_{-\infty}^{\infty} dy [x^2 + P^2(y + \mu)^2] W_n(k_0 x, k_0 y, -\Upsilon k_0 b_3) \cdot \exp(-i\eta_x x - i\eta_y y), \end{aligned} \quad (8)$$

where  $b_3 = [1 + P\Gamma(y + \mu)]x^2 + P\Gamma y^3 + P(P + 3\Gamma\mu)y^2 + P\mu(P + 2\Gamma\mu)y$ ,  $\eta_x = k_0\rho_x$ ,  $\eta_y = k_0\rho_y$ ;  $x = k_x/k_0$  and  $y = k_y/k_0$  are non-dimensional wave parameters. The double integral in Equation (8) depends only on the shape of the fluctuation spectrum but not on the strength of the fluctuations. Phase fluctuations at different observation points are not independent but correlate, and the asterisk represents the complex conjugate.

The phase wave structure function and the angles of arrival of scattered electromagnetic waves in the main and perpendicular planes can be easily calculated using Equations (7) and (8) [1, 15]:

$$\begin{aligned} D_1(\mathbf{r}_1, \mathbf{r}_2) &= \langle (\varphi_1(\mathbf{r}_1) - \varphi_1(\mathbf{r}_2)) (\varphi_1^*(\mathbf{r}_1) - \varphi_1^*(\mathbf{r}_2)) \rangle, \\ \langle \Theta_x^2 \rangle &= \lim_{\eta_x \rightarrow 0} \frac{D_1(\eta_x, 0, L)}{\eta_x^2}, \quad \langle \Theta_y^2 \rangle = \lim_{\eta_y \rightarrow 0} \frac{D_1(0, \eta_y, L)}{\eta_y^2}. \end{aligned} \quad (9)$$

Correlation function of the complex field in the collisionless magnetized plasma can be written as [16, 17]:

$$\begin{aligned} W_E(\rho_x, \rho_y, z) &\equiv \langle E(x + \rho_x, y + \rho_y, z) E^*(x, y, z) \rangle \\ &= E_0^2 \exp(ik_y \rho_y) \langle \exp\{i\varphi_1(x + \rho_x, y + \rho_y, z) - i\varphi_1^*(x, y, z)\} \rangle. \end{aligned} \quad (10)$$

In the most interesting case of multiple scattering, when phase fluctuations are strong  $\langle \phi_1 \phi_1^* \rangle \gg 1$ , we can assume that they obey a normal distribution [1, 2]. Correlation function decreases sharply as  $\rho_x$  and  $\rho_y$  increase, and the argument of the second exponential term can be expanded in a series [16, 17]:

$$W_E(\rho_x, \rho_y, z) = E_0^2 \exp(ik_y \rho_y) \exp\left(\frac{\partial V_\varphi}{\partial \rho_y} \rho_y + \frac{1}{2} \frac{\partial^2 V_\varphi}{\partial \rho_x^2} \rho_x^2 + \frac{1}{2} \frac{\partial^2 V_\varphi}{\partial \rho_y^2} \rho_y^2\right), \quad (11)$$

where the phase correlation function  $V_\varphi$  is given by Equation (8). The derivatives of the phase correlation function are taken at the point  $\rho_x = \rho_y = 0$ .

The 2D spatial power spectrum (SPS) of scattered radiation which is of great practical importance can be obtained by Fourier transformation from the correlation function in Eq. (11) [1, 2]:

$$S(k_x, k_y, z) = \frac{1}{(2\pi)^2} \int_{-\infty}^{\infty} d\rho_x d\rho_y W_E(\rho_x, \rho_y, z) \exp(-ik_x \rho_x - ik_y \rho_y). \quad (12)$$

This characteristic is equivalent to the ray intensity (brightness), which usually enters the radiation transport equation [1, 2]. In the most interesting case of strong fluctuation of the phase  $\langle \varphi_1 \varphi_1^* \rangle \gg 1$ , SPS is expressed as follows [16, 17]:

$$S(k_x, k_y, z) = S_0 \exp\left[-\frac{k_x^2}{2\langle k_x^2 \rangle} - \frac{(k_y - \Delta k_y)^2}{2\langle k_y^2 \rangle}\right], \quad (13)$$

where  $S_0$  is the peak value of the spectral curve, and  $\Delta k_y$  determines the displacement of the SPS of the received radiation caused by random plasma irregularities, while  $\langle k_x^2 \rangle$  and  $\langle k_y^2 \rangle$  determine the widths of this spectrum in the  $XZ$  and  $YZ$  planes, respectively. The expressions  $\Delta k_y$  and  $\langle k_y^2 \rangle$  may be obtained directly from Equation 8) by differentiation. Similar calculations can be carried out for  $\langle k_x^2 \rangle$  taking into account the fact that the observation points are spaced at small distance apart in the  $YZ$  plane near the point  $y = 0$ . As a result, we have obtained:

$$\Delta k_y = \frac{1}{i} \frac{\partial V_\varphi}{\partial \rho_y}, \quad \langle k_y^2 \rangle = -\frac{\partial^2 V_\varphi}{\partial \rho_y^2}, \quad \langle k_x^2 \rangle = -\frac{\partial^2 V_\varphi}{\partial \rho_x^2}. \quad (14)$$

The derivatives of the correlation function of the complex phase fluctuations are taken at the point  $\rho_x = \rho_y = 0$ . The parameter range in which expressions (13) and (14) correctly describe the SPS of scattered radiation is determined by the following inequalities [18]:  $|\Delta k_x| \ll 2\pi/\lambda$ ,  $\sqrt{\langle k_x^2 \rangle} \ll 2\pi/\lambda$ ,  $\sqrt{\langle k_y^2 \rangle} \ll 2\pi/\lambda$ . These conditions are not in contravention to the assumption of strong phase fluctuations because in a smoothly inhomogeneous medium mean spatial scale of plasma irregularities of the phase correlation function substantially exceeds the wavelength of scattered electromagnetic waves,  $l \gg \lambda$  ( $l$  is characteristic spatial scale of plasma irregularities caused by electron density fluctuations) [2], and the angle of the normal to the random wavefront  $\Delta\theta \sim \lambda\sqrt{\langle \varphi_1^2 \rangle}/l$  can remain small even at  $\langle \phi_1^2 \rangle \gg 1$ . Further we will consider only electron density fluctuations in  $F$  region of the ionosphere.

Ionospheric phase scintillation fluctuations are characterized by the scintillation index. For weak scattering of electromagnetic waves the scintillation level  $S_4$  and the 2D phase spectral function describing 2D diffraction pattern at the ground are connected by the relationship [19]:

$$S_4^2 = 4k_0^2 \int_{-\infty}^{\infty} dx \int_{-\infty}^{\infty} dy V_\varphi(x, y, L) \sin^2 [\Lambda_f^2 (x^2 + y^2)], \quad (15)$$

where  $\Lambda_f = k_0/k_f$ ,  $k_f = (4\pi/\lambda L)^{1/2}$  is the Fresnel wavenumber,  $\lambda$  the wavelength of an incident wave,  $L$  a mean distance between the observer and plasma irregularities, and  $(\lambda L)^{1/2}$  the Fresnel radius. The sinusoidal term is responsible for oscillations in the scintillation spectrum. The spatial autocorrelation function of the diffraction pattern could be measured with a suitable two-dimensional array of sensors.

Satellite and/or the  $F$ -region plasma irregularities moving relative to the receiver, temporal variations of intensity and phase are recorded. We assume that irregularities drift across the beam of the radio signals without changing their shapes (the assumption of “frozen-in” irregularities) along the  $X$ -axis with apparent velocity  $V_x$  transverse to the line of the sight path. The power spectrum  $P_S(\nu, L)$ , scintillation level  $S_4$  (zero moment) and spectral width (1st and square root 2nd moments) are computed from the power spectrum (one-dimensional case) [20]

$$P_\varphi(\nu, L) = \frac{2\pi}{V_x} \int_0^\infty dk_x W_\varphi \left( k_x = \frac{2\pi\nu}{V_x}, k_y, L \right), \quad P_S(\nu, L) = 4P_\varphi(\nu, L) \sin^2 \left( \frac{\nu}{\nu_f} \right)^2, \quad (16)$$

$$S_4^2 = \int_0^\infty d\nu P_S(\nu, L), \quad \nu_{1S} = \frac{1}{S_4^2} \int_0^\infty d\nu \nu P_S(\nu, L), \quad \nu_{2S} = \frac{1}{S_4} \left[ \int_0^\infty d\nu \nu^2 P_S(\nu, L) \right]^{1/2}. \quad (17)$$

The Fresnel frequency  $\nu_f = V_x/(\pi\lambda L)^{1/2}$  is directly proportional to the drift velocity  $V_x$  of plasma irregularities normal to the  $YZ$  plane and inversely proportional to the Fresnel radius, and  $\nu$  is the scintillation frequency.

#### 4. NUMERICAL CALCULATIONS

The incident electromagnetic wave having frequency of 3 MHz ( $k_0 = 6.28 \cdot 10^{-2} \text{m}^{-1}$ ) propagates along the  $Z$ -axis. Plasma parameters at the altitude of 300 km are:  $u_0 = 0.22$ ,  $v_0 = 0.28$ . The first Fresnel radius and Fresnel wavenumber are equal to 5.5 km and  $0.64 \text{km}^{-1}$ , respectively.

The observations of an RH-560 rocket flight from Sriharikota rocket range (SHAR), India ( $14^\circ\text{N}$ ,  $80^\circ\text{E}$ , dip latitude  $5.5^\circ\text{N}$ ; apogee was 348 km) show [21] that the intermediate range irregularities (100 m–2 km) were observed in abundance in altitude regions 220–250 km and 290–320 km. Irregularities of a range of scale sizes starting from a few hundred meters to a few tens of kilometers are observed in these patches.

Data obtained from spaced receiver measurements made at Kingston, Jamaica (during the periods August 1967–January 1969 and June 1970–September 1970) show that the irregularities between heights of 153 and 617 km causing the scintillation of signals from the moving earth satellites (BE-B and BE-C) are closely aligned along the magnetic field lines in the  $F$ -region of the ionosphere [22]. The dip angle

of the irregularities with respect to the field lines was within  $16^\circ$ . The anisotropic spectral features in the  $F$ -region are defined for the Gaussian and Power-law spectra.

Observations (Tbilisi,  $41^\circ 43\text{N}$ ) of drift small-scale irregularities in the ionospheric  $F$ -region show [23] that they have elliptic forms, and the ratio of axes basically varies from 1 to 3. Anisotropy axis is mainly oriented along the geomagnetic field of lines. Drift of small-scale irregularities mainly has S-W direction. The most probable values of drift velocity is in the range of 40–100 meter/sec.

Measurements of satellite's signal parameters moving in the ionosphere show that in  $F$ -region of the ionosphere irregularities have power-law spectrum. 3D power-law spectral correlation function of electron density irregularities with a power-law index  $p$  has been proposed in [24, 25]. The corresponding spectral function has the form:

$$W_n(\mathbf{k}) = \frac{\sigma_n^2}{(2\pi)^{3/2}} \frac{r_0^3 (k_0 r_0)^{(p-3)/2}}{\left(r_0 \sqrt{k^2 + k_0^2}\right)^{p/2}} \frac{K_{p/2}(r_0 \sqrt{k^2 + k_0^2})}{K_{(p-3)/2}(k_0 r_0)}, \quad (18)$$

where  $\sigma_n^2$  is the mean-square fractional deviation of electron density,  $K_\nu(x)$  the McDonald function,  $p$  the power index,  $r_0$  the inner scale of turbulence, and  $L_0 = 2\pi/k_0$  the outer scale; it is supposed that  $k_0 r_0 \ll 1$ . In the interval of wavenumber  $k_0 r_0 \ll k r_0 \ll 1$  spatial spectrum can be written as [24, 25]:

$$W_n(\mathbf{k}) = \frac{\sigma_n^2}{(2\pi)^{3/2}} \frac{\Gamma(p/2)}{\Gamma[(p-3)/2]} \frac{k_0^{p-3}}{(k^2 + k_0^2)^{p/2}},$$

where  $\Gamma(x)$  is the gamma function.

We will use new spectrum of electron density irregularities combining anisotropic Gaussian and power-law spectra [8]:

$$W_n(\mathbf{k}) = \frac{\sigma_n^2}{8\pi^{5/2}} \frac{A_p l_{\parallel}^3}{\chi^2 \left[1 + l_{\perp}^2 (k_x^2 + k_y^2) + l_{\parallel}^2 k_z^2\right]^{p/2}} \exp\left(-\frac{k_x^2 l_{\perp}^2}{4} - p_1 \frac{k_y^2 l_{\parallel}^2}{4} - p_2 \frac{k_z^2 l_{\parallel}^2}{4} + p_3 k_y k_z l_{\parallel}^2\right), \quad (19)$$

where  $p_1 = (\sin^2 \gamma_0 + \chi^2 \cos^2 \gamma_0)^{-1} [1 + (\chi^2 - 1)^2 \sin^2 \gamma_0 \cos^2 \gamma_0 / \chi^2]$ ,  $p_2 = (\sin^2 \gamma_0 + \chi^2 \cos^2 \gamma_0) / \chi^2$ ,  $p_3 = (\chi^2 - 1) \sin \gamma_0 \cos \gamma_0 / 2\chi^2$ ,  $A_p = \Gamma(p/2) \Gamma[(5-p)/2] \sin[(p-3)\pi/2]$ ;  $k_x$ ,  $k_y$  and  $k_z$  are the wave vector  $\mathbf{k}$  components perpendicular ( $k_x, k_y$ ) and parallel ( $k_{\parallel}$ ) to the incident wave propagation;  $\chi = l_{\parallel} / l_{\perp}$  is the anisotropy factor — the ratio of longitudinal and transverse characteristic linear sizes of plasma irregularities;  $\gamma_0$  is the orientation angle of elongated ionospheric plasma irregularities with respect to the magnetic lines of force. The shape of electron density irregularities has a spheroidal form. Anisotropy of the shape of irregularities is connected with the difference of the diffusion coefficients in the field align and field perpendicular directions.

Experimental investigations of the Doppler frequency shift of ionospheric signal and measurement by translucence of satellite signals show that index of the power-law spectrum of electron density fluctuations is in the range of  $3.8 \leq p \leq 4.6$  ( $\langle p \rangle \approx 4$ ) [25]. Experimental observations of backscattering signals from the artificially disturbed region of the ionosphere by the powerful HF radio emission shows that a lot of artificial ionospheric irregularities of the electron density are stretched along the geomagnetic field. Power-law spectral index was within the limits  $p = 1.4 \div 4.8$  for different heating sessions using ‘‘Sura’’ heating facility in the frequency range of  $4.7 \div 9$  MHz (ordinary mode) with the effective radiated power  $50 \div 70$  MW beamed vertically upwards [26].

Scintillation spectra are in agreement with 3D power-law irregularity spectrum with an exponent around  $-4$  [25, 26]. This exponent of  $-4$  is in agreement with the in situ measurements of the one-dimensional irregularity spectrum derived from rockets and satellites.

Substituting Equation (19) into Equations (8) and (9) at  $p = 4$  the variance and correlation function of the phase fluctuations are:

$$\begin{aligned} \langle \varphi_1^2 \rangle &= \frac{\sigma_n^2 A^2 \xi^3 k_0 L}{4\pi \chi^2} \int_{-\infty}^{\infty} dx \int_{-\infty}^{\infty} dy \frac{[x^2 + P^2 (\mu^2 - y^2)] - 2iPxy}{[(1 + \xi^2 G_1) - i\xi^2 G_2]^2} \exp\left[-\frac{\xi^2}{4} (G_3 x^4 + G_4 x^2 + G_5)\right] \\ &\cdot \exp[-i\xi^2 (G_6 x^3 + G_7 x)], \end{aligned} \quad (20)$$

where:  $G_1 = \frac{2\Gamma\mu}{\mu^4 P^3} x^4 + (\frac{1}{\chi^2} + \frac{T_2}{\mu^4 P^4}) x^2 + (\frac{y^2}{\chi^2} + \frac{T_3}{\mu^4 P^4})$ ,  $T_2 = 2P^2 y^4 + 2P\Gamma\mu(1 - P^2)y^2 - P^2\mu^2$ ,  $T_3 = P^3[-2\Gamma y^4 + \mu^2(P + 2\Gamma\mu)^2 y^2]$ ,  $G_2 = \frac{2}{\mu^4 P^4}(-\Lambda_2 x^3 + \Lambda_3 x)$ ,  $\Lambda_2 = 2P[\Gamma^2 y^2 + \Gamma\mu(P - \Gamma\mu)]y$ ,  $\Lambda_3 = P[\Gamma^2 y^4 + 2\Gamma\mu(P - \Gamma\mu)y^2 + P\mu^2(P - 2\Gamma\mu)]y$ ,  $G_3 = \frac{2\Gamma\mu p_2}{\mu^4 P^3}$ ,  $G_4 = \frac{1}{\chi^2} + \frac{p_2 T_2}{\mu^4 P^4} + 4\frac{p_3 \Gamma}{\mu^2 P} y^2$ ,  $G_5 = \frac{4\Gamma p_3}{\mu^2 P} y^4 + [p_1 - \frac{4p_3}{\mu P}(P + 2\Gamma\mu)]y^2 - \frac{p_2 T_3}{\mu^4 P^4}$ ,  $G_6 = \frac{1}{\mu^2 P^2} (\frac{p_2 \Lambda_2}{2\mu^2 P^2} - \Gamma p_3 y)$ ,  $G_7 = \frac{1}{\mu^2 P^2} (\frac{p_2 \Lambda_3}{2\mu^2 P^2} - \Gamma p_3 y^3 + P p_3 \mu y)$ .

$$V_\varphi(\eta, L) = \frac{\sigma_n^2}{4\pi^{3/2}} \frac{A^2 A_p}{\chi^2} \xi^3 k_0 L \int_{-\infty}^{\infty} dx \int_{-\infty}^{\infty} dy \frac{x^2 + P^2(y + \mu)^2}{[1 + \frac{\xi^2}{\chi^2}(x^2 + y^2) + D_4]^2} \exp\left[-\frac{\xi^2}{4}(D_1 x^4 + D_2 x^2 + D_3)\right] \cdot \exp(-i\eta_x x - i\eta_y y), \quad (21)$$

where  $D_1 = \frac{p_2 C_0^2}{\mu^4 P^4}$ ,  $D_2 = \frac{1}{\chi^2} + \frac{2p_2 C_0}{\mu^4 P^4}(-C_3 y^3 + C_2 y^2 + C_1 y) + \frac{4p_3 C_0}{\mu^2 P^2} y$ ,  $D_3 = p_1 y^2 + \frac{1}{4\mu^2 P^2} \{ \frac{p_2}{\mu^2 P^2} [C_3^2 y^6 - 2C_2 C_3 y^5 + (C_2^2 - 2C_1 C_3) y^4 + 2C_1 C_2 y^3 + C_1^2 y^2] + 4p_3(-C_3 y^4 + C_2 y^3 + C_1 y^2) \}$ ,  $D_4 = \frac{\xi^2}{\mu^4 P^4} \{ C_0^2 x^4 + 2C_0(C_1 y + C_2 y^2 - C_3 y^3) x^2 + [C_3^2 y^6 - 2C_2 C_3 y^5 + (C_2^2 - 2C_1 C_3) y^4 + 2C_1 C_2 y^3 + C_1^2 y^2] \}$ ,  $b_3 = C_0 x^2 + C_3 y^3 + C_2 y^2 + C_1 y$ .

Figure 1 depicts the 3D normalized correlation function of the phase fluctuations when two observation points are located in mutually perpendicular planes at distances  $\eta_x$  and  $\eta_y$ ;  $\sigma_n = 10^{-3}$ , diffraction parameter  $\mu = 0.06$ , anisotropy factor  $\chi = 10$ , plasma irregularities are field aligned ( $\gamma_0 = 0^0$ ),  $\xi = 5(l_{\parallel} = 800 \text{ m})$ .

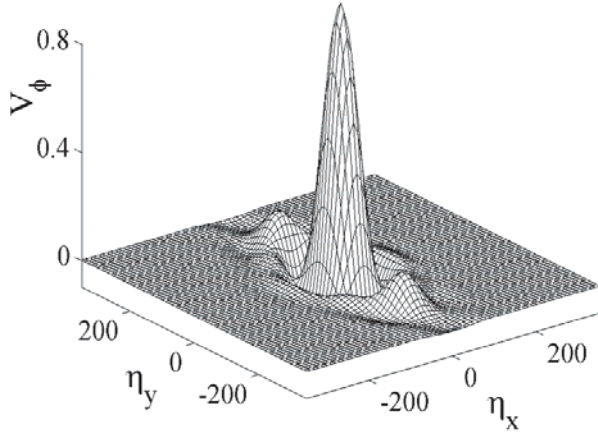


**Figure 1.** Normalized 3D correlation function of the phase fluctuations at  $\alpha = 60^\circ$ .

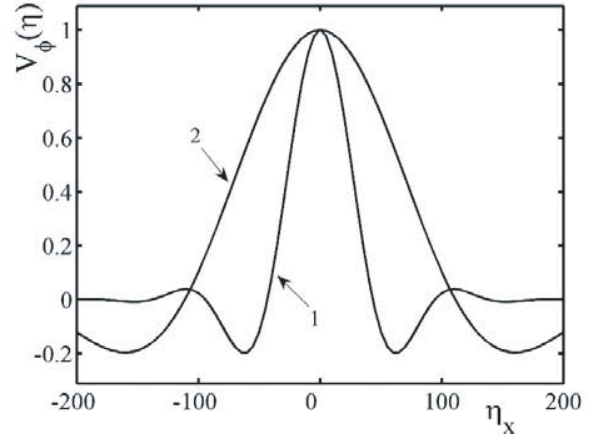


**Figure 2.** Normalized correlation function versus  $\eta_x$  for the extraordinary (curve 1) and the ordinary (curve 2) electromagnetic waves.

Figure 2 illustrates cross-sections of 3D phase correlation function (21) of the field aligned plasma irregularities in the main and perpendicular planes for both the ordinary and extraordinary waves (plasma parameters are the same as in Figures 1 and 2). The width of the curves is approximately the same in the main  $YZ$  plane (Figure 1) as the external magnetic field has similar influence on both waves. First and second minima are at  $\eta_y = 76$  and  $\eta_y = 80$ . In the  $XZ$  plane behaviors of these waves strongly differ. Broadening of the 2D correlation function for the ordinary wave 2.6 times exceeds the extraordinary one. Minima for the ordinary and extraordinary waves are at  $\eta_x = 160$  and  $\eta_x = 62$ , respectively.

From expressions (8) and (14) follows that the displacement  $\Delta k_x$  of the SPS in non-absorbing medium

(1) is equal to zero because the dependence on  $k_x$  is even. Plots of the parameter  $\Delta k_y$  as a function of anisotropy factor  $\chi$  for field aligned plasma irregularities are shown in Figure 3 at  $\xi = 5$ ,  $\mu = 0.06$ .

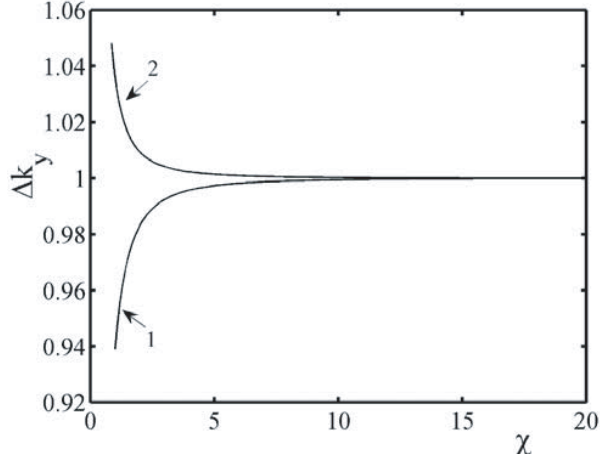


**Figure 3.** Plots of the displacement of the SPS as a function of anisotropy factor  $\chi$ .

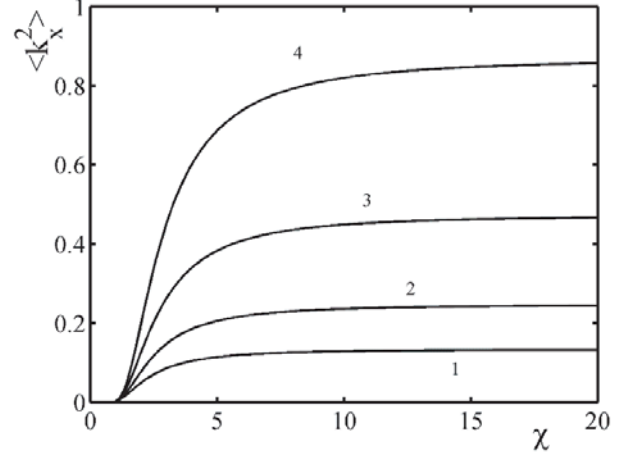


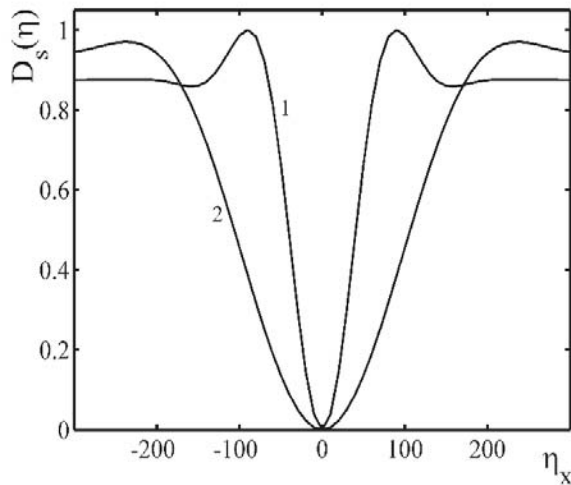
**Figure 4.** The width of the SPS in the  $XZ$  plane versus parameter  $\chi$  for the extraordinary wave.

Curve 1 corresponds to the extraordinary wave, and curve 2 is devoted to the ordinary wave. At small  $\chi < 10$  displacements of both waves are in opposite directions. Increasing anisotropy factor shift of these waves is the same in the  $YZ$  plane.

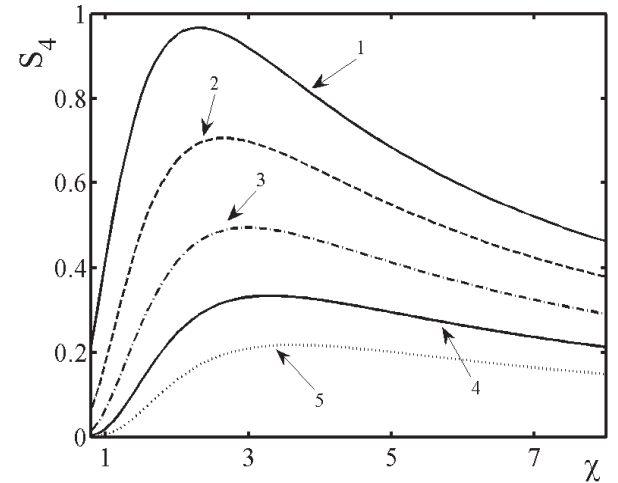
Figure 4 represents the broadening of the SPS of the extraordinary wave in the  $XZ$  plane at  $\xi = 100$ . Numerical calculations show that varying orientation angle in the interval  $\gamma_0 = 0^\circ \div 30^\circ$  the width of the SPS in the  $XZ$  plane exceeds the width in the  $YZ$  plane approximately three times.

Figure 5 depicts the phase structure function for the ordinary (curve 1) and extraordinary (curve 2) waves in the plane  $XZ$  at:  $\alpha = 60^\circ$ ,  $\xi = 10$ ,  $\chi = 10$ ,  $\gamma_0 = 0^\circ$ . Small-scale plasma irregularities having characteristic spatial scale 160 meters are field aligned. The width of the extraordinary wave exceeds the width of the ordinary wave 2.5 times. Curve 1 tends to saturation at  $\eta_x = 190$ , while curve 2 at  $\eta_y = 300$ . Phase structure function in the main plane oscillates having approximately the same widths.

Using Equation (9) phase structure function allows to calculate the angle-of-arrivals in the observation points in both  $XZ$  and  $YZ$  planes. Numerical calculations show that  $\langle \Theta_x^2 \rangle^{1/2} = 1.6' \div 0.4'$



**Figure 5.** Plots of the phase structure function versus distance between observation points in the  $XZ$  plane.



**Figure 6.** Scintillation index versus anisotropy factor  $\chi$  for different characteristic spatial scale of plasma irregularities.

at the anisotropy factor  $\chi = 1 \div 4$ , while  $\langle \Theta_y^2 \rangle^{1/2} = 0.7' \div 0.1'$  at  $\chi = 1 \div 3$ .

Scintillation effects are investigated for the parameters:  $\alpha = 60^\circ$ ,  $\sigma_n^2 = 3 \cdot 10^{-4}$ ,  $k_0 L = 10^5$  ( $L \approx 10^4$  km),  $\Lambda_f \approx 100$ . Figure 6 depicts curves of the phase scintillation index of the 3 MHz extraordinary wave scattered on elongated ( $\gamma_0 = 0^\circ$ ) ionospheric plasma irregularities. Scintillation index is maximum  $S_{4\max} = 0.97$  at  $\chi = 2.3$  if characteristic spatial scale of anisotropic inhomogeneities is equal to  $l_{\parallel} = 1.3$  km (curve 1)  $S_{4\max} = 0.7$  at  $\chi = 2.6$ ,  $l_{\parallel} = 1.6$  km (curve 2),  $S_{4\max} = 0.49$  at  $\chi = 3$ ,  $l_{\parallel} = 1.9$  km (curve 3),  $S_{4\max} = 0.33$  at  $\chi = 3.3$ ,  $l_{\parallel} = 2.2$  km (curve 4),  $S_{4\max} = 0.22$  at  $\chi = 3.7$ ,  $l_{\parallel} = 2.5$  km (curve 5). Scintillation level is varied between  $5 \cdot 10^{-3} \leq S_4 \leq 0.97$  for the anisotropy factor in the interval  $1 \leq \chi \leq 7$ . Hence, phase scintillation coefficient for small-scale plasma irregularities fastly increases; reaching maximum it slowly decreases inversely  $\delta$  proportional to the characteristic linear scale.

Figure 7 illustrates the behavior of the scintillation index of scattered extraordinary electromagnetic waves on the *F*-region anisotropic plasma irregularities having linear scale  $l_{\parallel} = 1.6$  km and different inclination angles to the external magnetic field. For elongated plasma irregularities ( $\gamma_0 = 0^\circ$ ) phase scintillation index reaches maximum  $S_{4\max} = 0.7$  at  $\chi = 2.6$  (curve 1), if  $\gamma_0 = 5^\circ$ ,  $S_{4\max} = 0.79$  at  $\chi = 2.7$  (curve 2), and if  $\gamma_0 = 15^\circ$ ,  $S_{4\max} = 0.94$  at  $\chi = 2.8$  (curve 3). Hence, scintillation index fastly grows in proportion to the orientation angle of elongated *F*-region ionospheric irregularities with respect to the external magnetic field in the interval  $1 \leq \chi \leq 3$ .

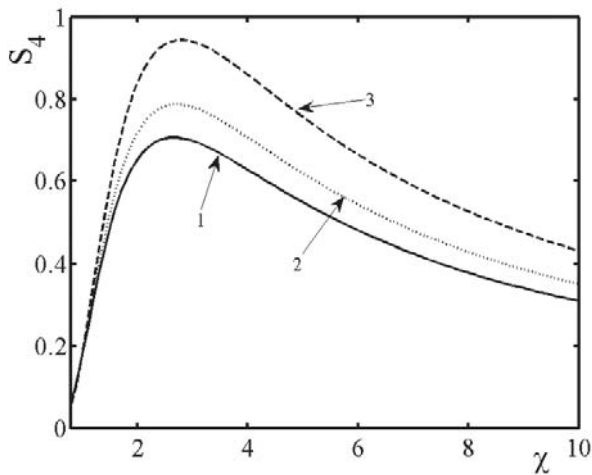


**Figure 7.** Scintillation index versus anisotropy factor  $\chi$  for different orientation angle of anisotropic plasma irregularities.

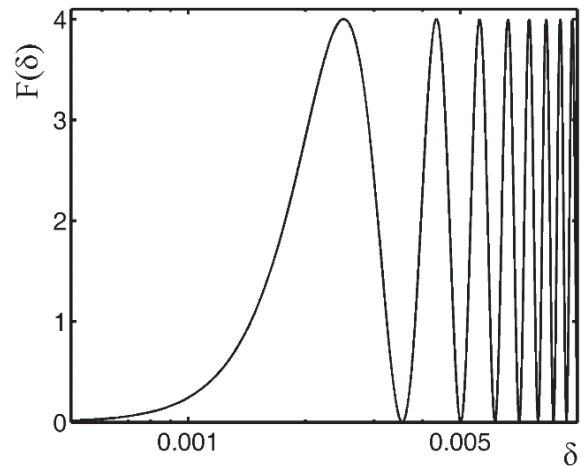
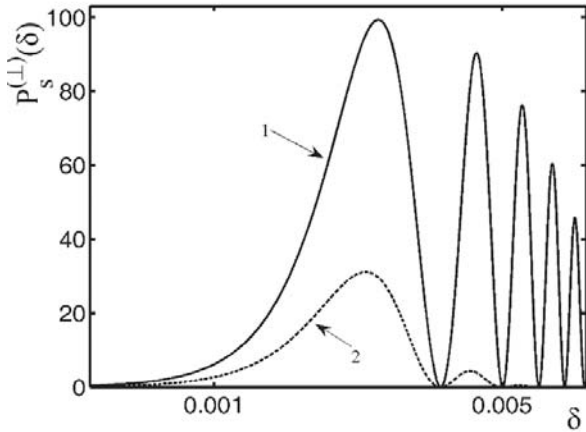


**Figure 8.** Fresnel filtering factor.

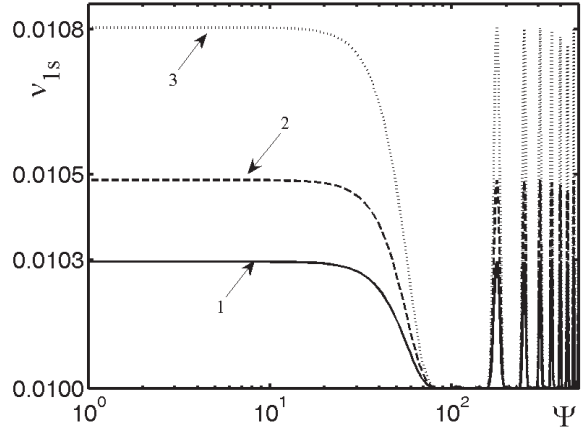
In Figures 6 and 7 phase scintillation index  $S_4$  slowly decreases inversely proportional to the anisotropy factor  $\chi$ . Low level scintillation is related with  $S_4 \leq 0.4$ , while  $S_4 \geq 0.4$  describes high scintillation level. According to [20], low scintillation level is associated with both positive and negative intensity fluctuations, and high levels correspond to the positive intensity fluctuations.

Figure 8 depicts semi-log curve representing oscillations of the Fresnel filtering factor  $F(\delta) = 4 \sin^2(\delta^2)$  versus parameter  $\delta = \nu/\nu_f$ . The oscillation minima appear with ratio 1:  $\sqrt{2} : \sqrt{3} : \sqrt{4} \dots$  (so called “standard relationship” [14]). Figure 9 illustrates semi-log plots of the power spectrum  $P_S^{(\pm)}(\nu, L)$  for both the ordinary (curve 1) and extraordinary (curve 2) waves versus parameter  $\delta$  at fixed:  $k_0 L = 60$  ( $L = 1$  km),  $V_x = 100$  m/sec,  $\mu = 0.06$ ,  $\alpha = 60^\circ$ ,  $\gamma_0 = 0^\circ$ ,  $\chi = 5$ ,  $\xi = 100$  ( $l_{\parallel} = 1.6$  km), the Fresnel frequency  $\nu_f = 10$  mHz. Minima of these curves satisfy the same condition.

Figure 10 depicts log-log plots of the spectral width of the power spectrum in Eq. (18) versus parameter  $\Psi = \nu_0/\nu_f$ ,  $\nu_0 = k_0 V_x/2\pi$ . Curve 1 corresponds to the field-aligned plasma irregularities ( $\gamma_0 = 0^\circ$ ), curve 2 —  $\gamma_0 = 20^\circ$ , curve 3 —  $\gamma_0 = 30^\circ$ . Breaking parameters are at:  $\Psi = 17$  (curve 1),  $\Psi = 19$  (curve 2),  $\Psi = 21$  (curve 3). The spectral width  $\nu_{1S}$  is approximately 10 mHz for 3 MHz incident



**Figure 9.** The power spectrum of the phase fluctuations versus parameter  $\delta$  for the ordinary and extraordinary waves.



**Figure 10.** The spectral width (1st moment) of the power spectrum for different orientation angle of elongated plasma irregularities.

electromagnetic wave. Scintillation period  $T_{1S} = 1/\nu_{1S}$  is of the order of 100 sec. Using Equation (17) numerical analyses show that  $\nu_{1S} < \nu_{2S} = 104$  mHz.

## 5. CONCLUSION

Statistical characteristics of scattered electromagnetic waves in the turbulent magnetized ionospheric plasma are calculated solving stochastic differential equation for the phase fluctuations taking into account boundary condition, diffraction effects and polarization coefficients for both ordinary and extraordinary waves. Variance and correlation function were obtained for arbitrary correlation function of electron density fluctuations. These second order statistical moments allow to estimate the broadening and shift of maximum of the SPS of scattered radiation, and also investigate scintillation effects in the F region of the ionosphere using the experimental data. Numerical calculations are carried out for 3 MHz incident wave and 3D anisotropic spectral function of electron density fluctuations characterizing anisotropic plasma irregularities containing both anisotropy factor and orientation angle of elongated plasma irregularities with respect to the external magnetic field.

It is shown that displacement and width of the SPS for the ordinary and extraordinary waves tends to the saturation increasing anisotropy factor. Shift of maximum of the SPS strongly depends on the orientation angle of anisotropic plasma irregularities particularly, and varying angle in the interval  $0^\circ$ – $30^\circ$  displacement of its maximum increases six times. The angle-of-arrivals in the main plane is less than in normal direction.

Phase scintillation index for small-scale irregularities fast growth in proportion to the orientation angle and reaching maximum slowly decreases inversely proportional to the characteristic linear scale of plasma irregularities. Low level scintillations are associated with both positive and negative intensity fluctuations, while high levels primarily correspond to positive intensity fluctuations.

Sinusoidal oscillations are observed in the intensity spectrum and are attributed to a Fresnel filtering effect for plasma irregularities having characteristic spatial scale less than the Fresnel radius. These oscillations satisfy the “standard relationship”. Scintillation level allows calculating the spectral width (first  $\nu_{1S}$  and second  $\nu_{2S}$  moments), and computing the power spectrum and scintillation period. If “frozen-in” elongated irregularities drift along the  $X$ -axis with the velocity 100 m/sec, spectral width  $\nu_{1S} \sim 10$  mHz; period is 100 sec;  $\nu_{1S} < \nu_{2S} = 104$  mHz. If elongated plasma irregularities are moving along the  $Y$ -axis,  $T_{1S} \sim 80$  sec and  $\nu_{1S} < \nu_{2S} = 118$  mHz. Knowledge data of these oscillations allow to calculate the velocity of plasma irregularities in the principal and perpendicular planes, to estimate characteristic spatial scales and the r.m.s. electron density fluctuations for plasma irregularities smaller than the Fresnel radius.

## ACKNOWLEDGMENT

The work has been supported by the International Science and Technology Center (ISTC) under Grant # G-2126 and Shota Rustaveli National Science Foundation under Grant # FR/3/9-190/14.

## REFERENCES

1. Ishimaru, A., *Wave Propagation and Scattering in Random Media. Vol. 2, Multiple Scattering, Turbulence, Rough Surfaces and Remote Sensing*, Academic Press, New York-San Francisco-London, 1978.
2. Rytov, S. M., Yu. A. Kravtsov, and V. I. Tatarskii, *Principles of Statistical Radiophysics. Vol. 4, Waves Propagation through Random Media*, Springer, Berlin, New York, 1989.
3. Wernik, A. W., J. A. Secan, and E. J. Fremouw, "Ionospheric irregularities and scintillation," *Advances Space Research*, Vol. 31, No. 4, 971–981, 2003.
4. Z.-W. Xu, J. Wu, and Z.-S. Wu, "A survey of ionospheric effects on space-based radar," *Waves in Random Media*, Vol. 14, 189–273, 2004.
5. Aarons, J., "Global morphology of ionospheric scintillation," *Proc. IEEE*, Vol. 70, 360–378, 1982.
6. Yeh, K. C. and C. H. Liu, "Radio wave scintillations in the ionosphere," *Proc. IEEE*, Vol. 70, 324–360, 1982.
7. Jandieri, G. V., A. Ishimaru, V. G. Jandieri, A. G. Khantadze, and Zh. M. Diasamidze, "Model computations of angular power spectra for anisotropic absorptive turbulent magnetized plasma," *Progress In Electromagnetics Research*, Vol. 70, 307328, 2007.
8. Jandieri, G. V., Zh. M. Diasamidze, and M. R. Diasamidze, "Scintillation spectra of scattered electromagnetic waves in turbulent magnetized plasma," *Journal of Basic and Applied Physics*, Vol. 2, 224–234, 2013.
9. Jandieri, G. V., Zh. M. Diasamidze, and M. R. Diasamidze, "Scintillation effects and the spatial power spectrum of scattered radio waves in the ionospheric F region," *Journal of Advances in Physics*, Vol. 13, 4593–4604, 2017.
10. Jandieri, G. V., Zh. M. Diasamidze, M. R. Diasamidze, and I. G. Takidze, "Second order statistical moments of the power spectrum of ionospheric scintillation," *Earth Science*, Vol. 6, 142–148, 2017.
11. Jandieri, G., A. Ishimaru, B. Rawat, O. Kharshiladze, and Zh. M. Diasamidze, "Power spectra of ionospheric scintillation," *Advanced Electromagnetics*, Vol. 6, 42–51, 2017.
12. Ginzburg, V. L., *Propagation of Electromagnetic Waves in Plasma*, Gordon and Beach, New York, 1961.
13. Jandieri, G. V., A. Ishimaru, N. F. Mchedlishvili, and I. G. Takidze, "Spatial power spectrum of multiple scattered ordinary and extraordinary waves in magnetized plasma with electron density fluctuations," *Progress In Electromagnetics Research M*, Vol. 25, 87–100, 2012.
14. Jandieri, G. V. and A. Ishimaru, "Some peculiarities of the spatial power spectrum of scattered electromagnetic waves in randomly inhomogeneous magnetized plasma with electron density and external magnetic field fluctuations," *Progress In Electromagnetics Research B*, Vol. 50, 77–95, 2013.
15. Jandieri, G. V., "“Double-humped effect” in the turbulent collision magnetized plasma," *Progress In Electromagnetics Research M*, Vol. 48, 95–102, 2016.
16. Gershman, B. N., L. M. Eruxhimov, and Yu. Ya. Yashin, *Wavy Phenomena in the Ionosphere and Cosmic Plasma*, Moscow, Nauka, 1984 (in Russian).
17. Gavrilenko, V. G., A. A. Semerikov, and G. V. Jandieri, "On the effect of absorption on multiple wave-scattering in magnetized turbulent plasma," *Waves in Random Media*, Vol. 9, 427–440, 1999.
18. Gavrilenko, V. G., A. V. Sorokin, G. V. Jandieri, and V. G. Jandieri, "Some properties of the angular power distribution of electromagnetic waves multiply scattered in a collisional magnetized plasma," *Plasma Physics Report*, Vol. 31, 604–615, 2005.

19. Bowhill, S. A., "Statistics of a Dario wave diffracted by a random ionosphere," *J. Res. Nat. Bur. Stand. Sect. D*, Vol. 65D, No. 3, 275–292, 1961.
20. Rufenach, C. L., "Power-law wavenumber spectrum deduced from ionospheric scintillation observations," *Journal of Geophysical Research*, Vol. 77, 4761–4772, 1972.
21. Raizada, S. and H. S. S. Sinha, "Some new features of electron density irregularities over SHAR during strong spread F," *Ann. Geophysicae*, Vol. 18, 141–151, 2000.
22. Chen, A. A. and G. S. Kent, "Determination of the orientation of ionospheric irregularities causing scintillation of signals from earth satellites," *Journal of Atmospheric and Terrestrial Physics*, Vol. 34, 1411–1414, 1972.
23. Kvavadze, N. D., Z. L. Liadze, N. V. Mosashvili, and Z. S. Sharadze, "The phenomenon of F-scattering and drift of small-scale irregularities at night low latitudes F-region of an ionosphere," *Geomagnetizm and Aeronomy*, Vol. 28, 139–141, 1988.
24. Shkarofsky, I. P., "Generalized turbulence space-correlation and wave-number spectrum-function pairs," *Canadian Journal of Physics*, Vol. 46, 2133–2153, 1968.
25. Kung, C. Y. and C.-H. Liu, "Radio wave scintillations in the ionosphere," *IEEE Proceedings*, Vol. 70, 324–360, 1982.
26. Bakhmet'eva, N. V., V. N. Bubukina, Yu. A. Ignat'ev, G. S. Bochkarev, V. A. Eremenko, V. V. Kol'sov, I. V. Krasheninnikov, and Yu. N. Cherkashin, "Investigation by backscatter radar irregularities produced in ionospheric plasma heating experiments," *Journal of Atmospheric and Terrestrial Physics*, Vol. 59, 2257–2263, 1997.